

論文 / 著書情報  
Article / Book Information

Title	Sub-Millimeter Pitch Multipole Magnetization in a Sintered Nd-Fe-B Magnet Utilizing Laser Heating
Author	Ryogen Fujiwara, Shunya Tanaka, Wataru Hijikata, Tadahiko Shinshi
Journal/Book name	IEEE MAGNETICS LETTERS, Volume 7, ,
Issue date	2016, 2
DOI	<a href="http://dx.doi.org/10.1109/LMAG.2015.2508004">http://dx.doi.org/10.1109/LMAG.2015.2508004</a>
URL	<a href="http://www.ieee.org/index.html">http://www.ieee.org/index.html</a>
Copyright	(c)2016 IEEE. Personal use of this material is permitted. Permission from IEEE must be obtained for all other users, including reprinting/republishing this material for advertising or promotional purposes, creating new collective works for resale or redistribution to servers or lists, or reuse of any copyrighted components of this work in other works.
Note	このファイルは著者（最終）版です。 This file is author (final) version.

Title:

Sub-millimeter pitch multi-pole magnetization of a sintered Nd-Fe-B magnet utilizing laser heating

Authors:

Ryogen Fujiwara<sup>1,2</sup>, Shunya Tanaka<sup>1</sup>, Wataru Hijikata<sup>3</sup>, Tadahiko Shinshi<sup>3,\*</sup>

<sup>1</sup> Interdisciplinary Graduate School of Science and Engineering, Tokyo Institute of Technology, Yokohama, Japan

<sup>2</sup> Research Fellow of Japan Society for the Promotion of Science, Japan

<sup>3</sup> Precision and Intelligence Laboratory, Tokyo Institute of Technology, Yokohama, Japan

Abstract:

Sub-millimeter pitch multi-pole magnetization of a sub-mm thick sintered Nd-Fe-B magnet is discussed in this paper. In this magnetization technique, some parts of a uniformly magnetized Nd-Fe-B magnet are heated by laser beam scanning, and the heated parts, in which the coercivity is weakened, are reverse-magnetized by the leakage flux generated from the adjacent non-heated magnets. To realize a high aspect magnetization by limiting the heated area, slits are processed in a substrate consisting of a magnet and a glass plate. The slit depth and the laser scanning condition were determined by simulating the temperature distribution in the magnet. A 500  $\mu\text{m}$  thick magnet was multipole-magnetized with a 650  $\mu\text{m}$  pitch, and the newly magnetized magnet generated a vertical magnetic field of 0.48 T (p-p) at a distance of 100  $\mu\text{m}$  from the surface, which is 90% of that of a simulated version.

Index terms:

Magnetic Instruments, MEMS, multi-pole magnetization, sintered Nd-Fe-B magnet

## 1. INTRODUCTION

Multi-pole magnetization of a flat permanent magnet is an important technology to decrease the demagnetization field by increasing the aspect ratio (magnetized width-to-thickness) and to realize a complicated magnetic flux flow. To date, nanometer- and micrometer-scale multi-pole magnetization has been realized by utilizing laser heating [Imamura 1980, Fujiwara 2014] for permanent magnet films of less than several micrometers in thickness [Martens 1985, Uehara 2005]. However, in the case of sintered Nd-Fe-B magnets, sub-millimeter pitch multi-pole magnetization has not been realized, although multi-pole magnetization with a 2 mm pitch was realized by utilizing pulse

magnetization [Töpfer 2004]. Sub-millimeter pitch multi-pole sintered Nd-Fe-B magnets are a promising flux source for micro actuators fabricated using microelectromechanical systems (MEMS) technology due to their superior magnetic properties and large volume. In this paper, we examined the sub-millimeter pitch multi-pole magnetization of sub-mm thick sintered Nd-Fe-B magnets utilizing laser heating. To realize a high aspect magnetization, we proposed a partial heating method by processing slits. The slit depth and the laser scanning condition were determined by simulating the temperature distribution in the magnet.

## 2. MAGNETIZATION METHOD

### A. Overview of Magnetization Process

The sub-millimeter pitch multi-pole magnetization process is shown in Fig. 1. First, a sintered Nd-Fe-B magnet is bonded on a glass plate. Secondly, some slits are processed as heat insulators in a subsequent process. Thirdly, after uniform and vertical magnetization, each divided magnet segment was alternately heated by laser beam scanning. The processed slit and the glass have low thermal conductivity, which limit unnecessary heat conduction. The heated parts in which the coercivity is weakened are reverse-magnetized by the leakage flux generated from non-heated adjacent magnets. Compared to conventional magnetization using laser heating [Fujiwara 2014], the magnet thickness is about 100 times greater than the sputtered film, and the heated part is limited by the slit, which can increase the aspect ratio and decrease the demagnetization field. Fig.2 shows the dimensions of the target magnetization of 500  $\mu\text{m}$  in width and 650  $\mu\text{m}$  in pole pitch.

### B. Material

An anisotropic sintered Nd-Fe-B magnet (Magfine Corp., NFB-N35) with dimensions of 10 mm  $\times$  10 mm  $\times$  0.5 mm is used as the substrate in this paper. This magnet has an easy magnetization axis in the out-of-plane direction. The residual magnetic flux density ( $B_r$ ) and coercivity ( $H_{cb}$ ) are 0.85 T and 610 kA/m, respectively. A glass plate (Schott AG, Tempax float) with dimensions of 10 mm  $\times$  10 mm  $\times$  0.7 mm is chosen as the supporting substrate because glass of low thermal conductivity is suitable for heating the magnet parts while minimizing thermal dissipation.

### C. Target Value of Heating Temperature

The magnetic flux density distribution generated by the non-heated magnet parts was calculated by using a magnetic field simulator (ANSYS, Maxwell 2D ver. 15) to

investigate the magnetic field applied to the heated part. Fig. 3 shows the analytical model, and Fig. 4 shows the simulated magnetic flux density distribution in the out-of-plane direction. This result shows that over 0.18 T is applied to the heated part.

To determine the target value of the heating temperature, the magnetization curve of the sintered Nd-Fe-B magnet was measured by VSM (Riken Denshi co., ltd., BHH-25) at 200°C and 300°C. Fig. 5 shows the measured curves. These results suggest that 1) 200°C is insufficient to saturate the magnetization and to realize magnetization reversal by applying a magnetic field of 143 kA/m (0.18 T in air), and 2) the substrate is no longer ferromagnetic at 300°C and further heating has little influence on the magnetization. Therefore, the target value for the heating temperature was determined to be 300°C.

#### D. Bonding Method

The linear expansion coefficient perpendicular to the easy magnetization direction of a sintered magnet was measured to determine the bonding method. A sintered Nd-Fe-B magnet with dimensions of 20 mm × 5 mm × 3 mm (Magfine Corp., NFB-N35) was used. Fig. 6 shows the result as measured by a thermomechanical analyzer (Rigaku Corp., Thermo plus EVO2 / TMA8310). Because the measured linear expansion coefficient is totally different from that of glass, at 3 – 3.3 ppm/K, thermal stress is generated at the interface during the laser heating. To buffer the thermal stress at the interface and to maintain bonding during laser heating, we chose heat-resistant polyimide as an adhesive. Both the magnet and the glass were spin coated (1600 rpm, 30 s) with a polyimide precursor solution (Toray Industries Inc., PW-1000). After baking (115°C, 3 min.), they were adhered by thermo-compression bonding (170°C, 1N, 30 min.).

#### E. Slit processing Method

A dicing saw (Disco corp., DAD321) with a 150 µm thick blade (Disco corp., P1A861 SDC320N50BR846 54×0.15×40) is used, and the magnet is sliced at a rotation speed of 20,000 rpm and a scanning speed of 2.0 mm/s with a scanning pitch of 650 µm. The slit depth is determined in the next section.

#### F. Heating Method

After uniform magnetization by applying a pulsed magnetic field with a maximum 4.7 T, the divided magnet was heated by a laser marker (Keyence Corp., MD-S9910) with a wavelength of 532 nm and a pulse repetition frequency of 30 kHz. To determine the slit depth and the laser scanning conditions, heat conduction during the laser heating was calculated using multiphysics simulation software (COMSOL AB, COMSOL

Multiphysics Ver. 4.4). The analytical models, the model conditions, and the physical properties are shown in Fig. 7, Table 1, and Table 2, respectively. Model A, B, C compares the effect of slit depth, and model C, D compares the effect of laser scanning conditions. In model A, B, C, a laser beam of 100 mm/s in speed scans the magnet 60 times, and in model D, a laser beam of 1.67 mm/s scans just once. The absorptivity of the laser beam was calculated from the measured reflectivity shown in Fig. 8, which was collected by a spectrophotometer (Shimadzu Scientific Instruments, Solidspec 3700DUV).

Fig. 9 shows a general view and a cross-sectional view of the temperature distributions at  $t=6$  s as simulated using model A, B, C. Though the input energy is the same, the temperature of the magnet only reached  $300^{\circ}\text{C}$  in model C. This result suggests that a deep slit is effective in order to heat the magnet while limiting unnecessary heat conduction. Fig. 10 (a) (b) shows the temperature distribution simulated using model D. On the one hand the temperature rise was insufficient at the cross-section point, as shown in Fig. 10 (a), but on the other hand, the temperature became too high close to the edge, as shown in Fig. 10 (b). A temperature of over  $600^{\circ}\text{C}$  exceeds the annealing temperature after sintering, so the maximum temperature should be limited to less than  $600^{\circ}\text{C}$  in order to avoid structural changes. In model C, the laser beam could heat the entire surface of the magnet uniformly, so the temperature reached  $300^{\circ}\text{C}$  without heating excessively, as shown in Fig. 10 (c). Therefore, we used the conditions of model C in the experiment.

### 3. MAGNETIZATION EVALUATION

Fig. 11 shows a photograph of a slotted magnet-glass substrate, where the white lines on the magnet indicate the trajectories of the focused scanning laser beam. Fig. 12 shows an expanded view of the slits. From these photographs, no detachment or damage to the magnet is observed.

In order to investigate the degradation of the magnetic properties due to bonding, slit processing and laser heating, demagnetization curves of unprocessed and processed magnets were measured by a VSM (Riken Denshi co., ltd., BHH-25) as shown in Fig. 13. There are no remarkable differences.

To clarify the sub-millimeter pitch multi-pole magnetization, the magnetic flux density distribution perpendicular to the magnet surface was measured by sliding a Hall element (Asahi Kasei Microdevices Corp., HG-0711) over the magnet. The Hall element has an active area of  $50\text{ }\mu\text{m} \times 50\text{ }\mu\text{m}$ , and the distance between the magnet surface and the active area is  $100\text{ }\mu\text{m}$ . Fig. 14 compares the measured magnetic flux density distribution with one simulated by three-dimensional magnetostatic analysis software

(ANSYS, Inc., Maxwell 3D Ver. 15). In the simulation, the magnet model shown in Fig. 2 was ideally magnetized. The magnetic properties measured by the unprocessed magnet shown in Fig. 13 were used. The measured magnetic field of 0.48 T (p-p) is about 90% of that of the simulated one. The reason for the imperfect magnetization should be investigated in the future.

#### 4. CONCLUSION

In this paper, we examined the sub-millimeter pitch multi-pole magnetization of a sub-mm thick sintered Nd-Fe-B magnet. In this magnetization, some parts of a uniformly magnetized Nd-Fe-B magnet are heated by a scanning laser beam, and the heated parts in which the coercivity is weakened are reverse-magnetized by the leakage flux generated from the adjacent non-heated magnets. To realize a high aspect magnetization by limiting the heated area, some slits are introduced into the magnet. A 500  $\mu\text{m}$  thick magnet was multipole-magnetized with a 650  $\mu\text{m}$  pitch, and the magnetized magnet generated a vertical magnetic field of 0.48 T (p-p) at a distance of 100  $\mu\text{m}$  from the surface, which is 90% of the simulated value. The magnetic properties were not significantly degraded due to these processes.

Future work is to perform perfect sub-millimeter pitch multi-pole magnetization, and to realize integrated micro magnetic MEMS devices utilizing this technology.

#### ACKNOWLEDGMENT

We are grateful to Dr. K. Suzuki and Dr. S. Kadota of TDK Corporation for providing useful advice. I want to thank Dr. T. Yoshino and Dr. M. Ebisawa of Tokyo Metropolitan Industrial Technology Research Institute for measuring the linear expansion coefficient and the reflectance of the sintered Nd-Fe-B magnet, respectively. This work was partly supported by TDK Corporation, JSPS KAKENHI Grant Number 26630036, Grant-in-Aid for JSPS Fellows Grant Number 14J00925.

#### REFERENCES

- Imamura N, Ota C (1980), "Experimental study on magneto-optical disk exerciser with the laser diode and amorphous magnetic thin films," *Japanese Journal of Applied Physics*, vol. 19, no. 12, pp. L731-L734, doi: 10.1143/JJAP.19.L731.
- Fujiwara R, Shinshi T, Kazawa E (2014), "Micromagnetization patterning of sputtered NdFeB/Ta multilayered films utilizing laser assisted heating," *Sensors and Actuators A: Physical*, vol. 220, pp. 298-304, doi: 10.1016/j.sna.2014.10.011.

Martens J, Voermans A (1984), "Cobalt ferrite thin films for magneto-optical recording," IEEE Transactions on Magnetics, vol. 20, no. 5, pp. 1007-1012, doi: 10.1109/TMAG.1984.1063167.

Uehara M, Gennai N, Fujiwara M, Tanaka T (2005), "Improved perpendicular anisotropy and permanent magnet properties in Co-doped Nd-Fe-B films multilayered with Ta," IEEE Transactions on Magnetics, vol. 41, no. 10, pp. 3838-3843, doi: 10.1109/TMAG.2005.854868.

Töpfer J, Christoph V (2004), "Multi-pole magnetization of NdFeB sintered magnets and thick films for magnetic micro-actuators," Sensors and Actuators A: Physical, vol. 113, no. 2, pp. 257-263, doi: 10.1016/j.sna.2004.04.011.

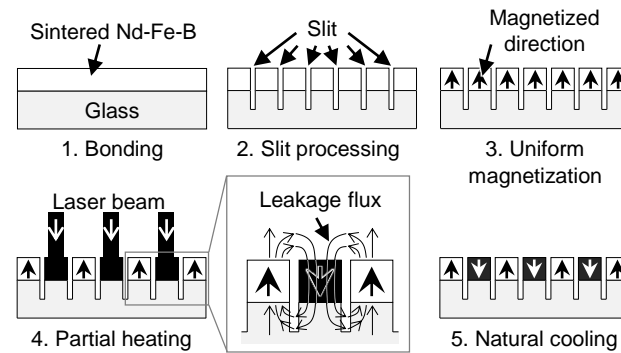


Fig. 1. Sub-millimeter pitch magnetization process



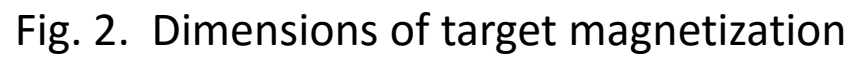


Fig. 2. Dimensions of target magnetization

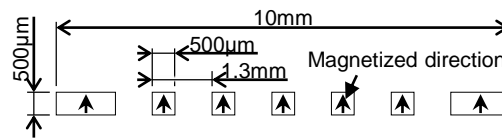


Fig. 3. Analytical model for investigating the magnetic field applied to the heating part

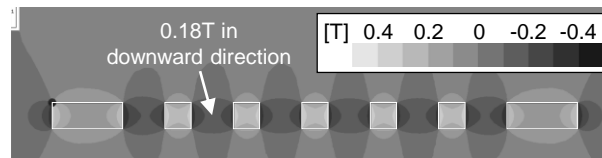


Fig. 4. Simulated magnetic flux density distribution in the out-of-plane direction generated by non-heated part

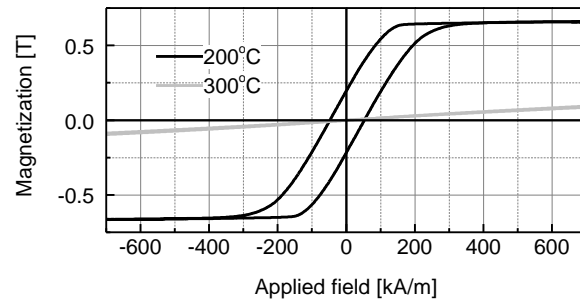


Fig. 5. Magnetization curves of the magnet at 200°C and 300°C

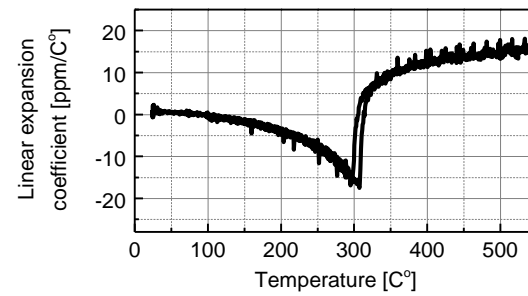


Fig. 6. Linear expansion coefficient perpendicular to the easy magnetization direction of a sintered Nd-Fe-B magnet

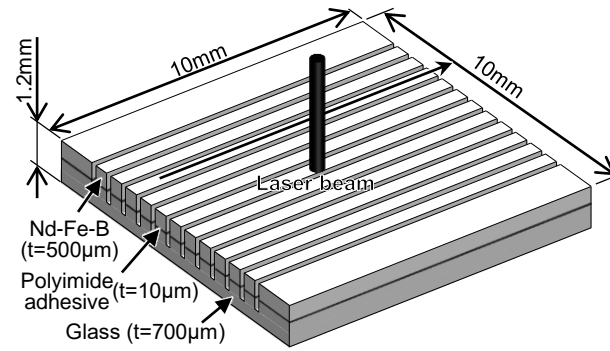


Fig. 7. Analytical model for heat conduction calculation (model C, D)

Table 1. Model conditions

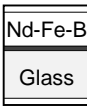
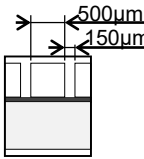
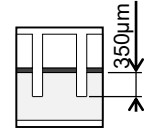
Model	A	B	C	D
Geometry				
Laser power		1.8 W		0.9 W
Intensity distribution		Gaussian distribution of 300 µm in spot diameter		
Absorptivity		90%		
Scanning speed		100 mm/s		1.67 mm/s
Number of scanning		60 times by intervals of 0.1026 s		1 time
Boundary conditions		Laser heating area: Constant heat flux Material interfaces: No contact resistance Other surfaces: Adiabatic		
Initial temperature		20°C		

Table 2. Physical properties

	Nd-Fe-B	Glass	Polyimide
Density (kg/m <sup>3</sup> )	7,600	2,200	1,420
Specific heat (J/kg·K)	500	900	500
Thermal conductivity (W/m·K)	9	1.2	0.16



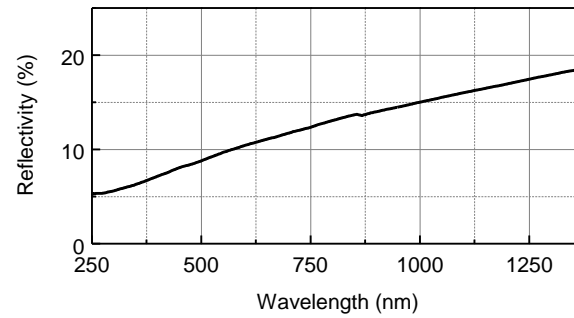


Fig. 8. Measured reflectivity of sintered Nd-Fe-B magnet

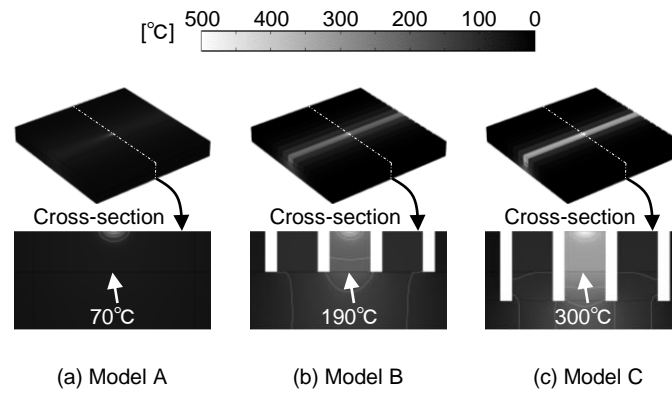


Fig. 9. Simulated temperature distribution at  $t=6$  s for determining the slit depth

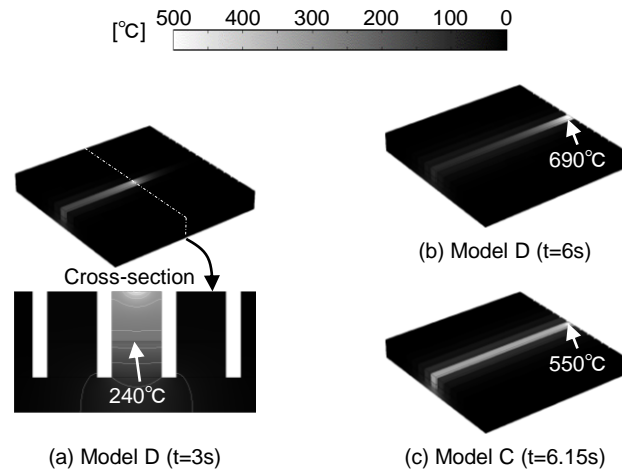


Fig. 10. Simulated temperature distribution for determining the laser scanning condition

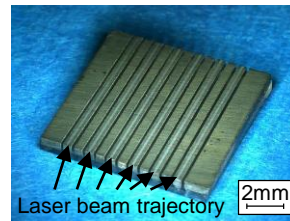


Fig. 11. Substrate after laser heating

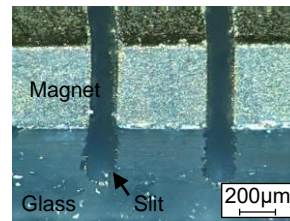


Fig. 12. Machined slits

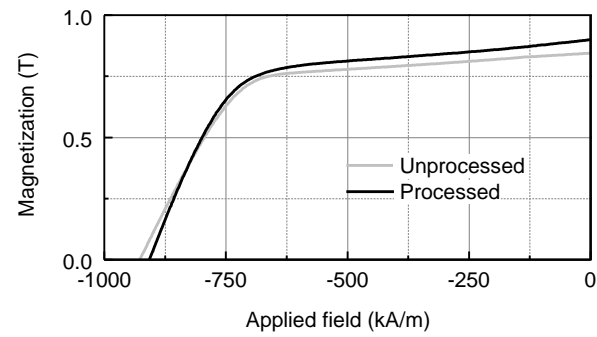


Fig. 13. Demagnetization curves

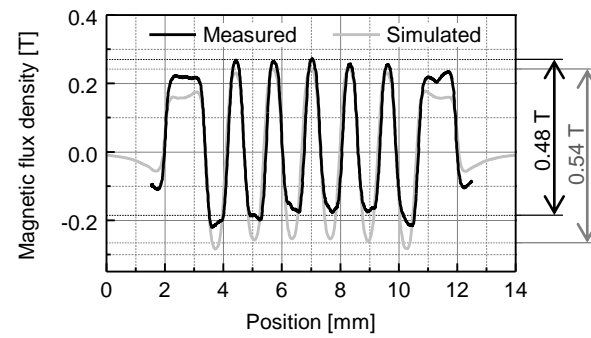


Fig. 14. Magnetic flux density distributions